

# blood

2005 106: 1113-1122  
Prepublished online Apr 26, 2005;  
doi:10.1182/blood-2005-02-0509

## **In vivo analyses of early events in acute graft-versus-host disease reveal sequential infiltration of T-cell subsets**

Andreas Beilhack, Stephan Schulz, Jeanette Baker, Georg F. Beilhack, Courtney B. Wieland, Edward I. Herman, Enosh M. Baker, Yu-An Cao, Christopher H. Contag and Robert S. Negrin

---

Updated information and services can be found at:

<http://bloodjournal.hematologylibrary.org/cgi/content/full/106/3/1113>

Articles on similar topics may be found in the following *Blood* collections:

[Transplantation](#) (1238 articles)

[Immunobiology](#) (3349 articles)

---

Information about reproducing this article in parts or in its entirety may be found online at:

[http://bloodjournal.hematologylibrary.org/misc/rights.dtl#repub\\_requests](http://bloodjournal.hematologylibrary.org/misc/rights.dtl#repub_requests)

Information about ordering reprints may be found online at:

<http://bloodjournal.hematologylibrary.org/misc/rights.dtl#reprints>

Information about subscriptions and ASH membership may be found online at:

<http://bloodjournal.hematologylibrary.org/subscriptions/index.dtl>

Blood (print ISSN 0006-4971, online ISSN 1528-0020), is published semimonthly by the American Society of Hematology, 1900 M St, NW, Suite 200, Washington DC 20036.

Copyright 2007 by The American Society of Hematology; all rights reserved.



# In vivo analyses of early events in acute graft-versus-host disease reveal sequential infiltration of T-cell subsets

Andreas Beilhack, Stephan Schulz, Jeanette Baker, Georg F. Beilhack, Courtney B. Wieland, Edward I. Herman, Enosh M. Baker, Yu-An Cao, Christopher H. Contag, and Robert S. Negrin

**Graft-versus-host disease (GVHD) is a major obstacle in allogeneic hematopoietic cell transplantation. Given the dynamic changes in immune cell subsets and tissue organization, which occur in GVHD, localization and timing of critical immunological events in vivo may reveal basic pathogenic mechanisms. To this end, we transplanted luciferase-labeled allogeneic splenocytes and monitored tissue distribution by in vivo biolumines-**

**cence imaging. High-resolution analyses showed initial proliferation of donor CD4<sup>+</sup> T cells followed by CD8<sup>+</sup> T cells in secondary lymphoid organs with subsequent homing to the intestines, liver, and skin. Transplantation of purified naive T cells caused GVHD that was initiated in secondary lymphoid organs followed by target organ manifestation in gut, liver, and skin. In contrast, transplanted CD4<sup>+</sup> effector memory T (T<sub>EM</sub>) cells did not proliferate in**

**secondary lymphoid organs in vivo and despite their in vitro alloreactivity in mixed leukocyte reaction (MLR) assays did not cause acute GVHD. These findings underline the potential of T-cell subsets with defined trafficking patterns for immune reconstitution without the risk of GVHD. (Blood. 2005;106:1113-1122)**

© 2005 by The American Society of Hematology

## Introduction

Allogeneic hematopoietic cell transplantation (HCT) has proven to be an effective therapy for a variety of life-threatening malignancies.<sup>1</sup> The beneficial effects of HCT are due to the graft-versus-tumor reaction, which is capable of destroying residual tumor cells that persist after chemotherapy or radiation therapy.<sup>2</sup> However, allogeneic HCT is limited by the immunologic recognition and destruction of host tissues, termed graft-versus-host disease (GVHD). Acute GVHD continues to be a major source of morbidity and mortality following HCT, which limits treatment of a broader spectrum of diseases, such as autoimmune diseases or organ transplant rejection.<sup>3,4</sup>

Tissue-specific destruction of GVHD target organs, as gastrointestinal tract, liver, and skin, underlines the importance of migration capacities of alloreactive T lymphocytes.<sup>5,6</sup> In the current study we aimed to determine the time points of organ infiltration and focused on the role of different lymphoid organs in initiating acute GVHD. We used in vivo bioluminescence imaging (BLI) to analyze the migration pattern of whole splenocytes after transplantation into allogeneic recipients. BLI has already proven to be a sensitive and accurate means of characterizing engraftment patterns of hematopoietic stem cells, of monitoring tumor cell growth, and of assessing response to conventional and biological therapies.<sup>7-9</sup>

We also aimed to clarify the role of different T-cell subsets during GVHD development. It is reported in the literature<sup>10-12</sup> that CD4<sup>+</sup> effector memory T (T<sub>EM</sub>) cells do not cause GVHD. This prompted us to characterize their trafficking and proliferation pattern in vivo, while comparing it to purified naive CD4<sup>+</sup> T lymphocytes.

## Materials and methods

### Mice

FVB/N (H-2<sup>q</sup>, Thy1.1) mice and Balb/c mice (H-2<sup>d</sup>, Thy1.2) were purchased from Jackson Laboratory (Bar Harbor, ME). The luciferase-expressing (*luc*<sup>+</sup>) transgenic FVB/N line was generated as previously described.<sup>9</sup> Female heterozygous *luc*<sup>+</sup> offspring of the transgenic founder line FVB-L2G85 were used for all transplantation experiments. All animal studies were performed under institutional approval.

### Flow cytometric cell purification and analysis

The following antibodies were purchased from BD Pharmingen (San Diego, CA) and eBiosciences (San Diego, CA) and used for fluorescence-activated cell-sorting (FACS) on an LSR flow cytometer (Becton Dickinson, Mountain View, CA): CD3ε (145-2c11), CD4 (RM4-5), CD8α

From the Departments of Medicine and Pediatrics, Stanford University, Stanford, CA.

Submitted February 23, 2005; accepted March 30, 2005. Prepublished online as *Blood* First Edition Paper, April 26, 2005; DOI 10.1182/blood-2005-02-0509.

A.B. and S.S. designed and performed research, contributed new reagents, analyzed data, and wrote the paper. J.B. and G.F.B. designed and performed research; C.B.W., E.I.H., and E.M.B. performed research and analyzed data; Y.A.C. contributed vital new reagents; C.H.C. designed research, contributed vital new reagents and analytical tools; and R.S.N. designed research and wrote the paper.

A.B. and S.S. contributed equally to this study.

Supported by a Supergen Postdoctoral Fellowship of the Amy Strelzer-Manasevit Research Program of the National Marrow Donor Program (NMDP) (A.B.), by an Amgen Oncology Fellowship (A.B.), by a fellowship of the

Akademie der Naturforscher Leopoldina (S.S.), and grants from the National Institutes of Health (R24CA92862, RO1CA80006, PO1CA49605, and R33CA88303).

C.H.C. is a scientific founder and consultant for Xenogen, and held his consulting position while this study was conducted. Xenogen manufactures and sells the low-light imaging instruments (IVIS) used in this study.

An Inside *Blood* analysis of this article appears in the front of this issue.

**Reprints:** Robert S. Negrin, Center for Clinical Sciences Research Building, Room 2205, 269 W Campus Dr, Stanford, CA 94305; e-mail: negrs@stanford.edu.

The publication costs of this article were defrayed in part by page charge payment. Therefore, and solely to indicate this fact, this article is hereby marked "advertisement" in accordance with 18 U.S.C. section 1734.

© 2005 by The American Society of Hematology

(53-6.7), CD11b/Mac-1 (M1/70), CD25 (PC61), CD44 (IM7), CD45R/B220 (RA3-6B2), CD62L (MEL14), CD69 (H1.2F3), Gr-1 (RB6-8C5), H-2K<sup>a</sup> (KH114), H-2D<sup>a</sup> (KH117), H-2D<sup>d</sup> (34-2-12), LPAM-1/α4β7 (DATK32), NK1.1 (PK136), Thy1.1 (H1S51), Thy1.2 (53-2.1). Dead cells were excluded by propidium iodide staining shortly before FACS.

For transplantation of T-cell subsets, splenic single-cell suspensions from FVB-L2G85 mice were enriched with CD4-conjugated magnetic beads using the AutoMACS system (Miltenyi Biotech, Auburn, CA). After a single enrichment step approximately 80% of splenocytes were CD4<sup>+</sup> before incubation with CD44–phycoerythrin (PE), CD62L–fluorescein isothiocyanate (FITC), and CD4–allophycocyanin (APC) and sorted into naive CD4<sup>+</sup> T cells (CD44<sup>-</sup>CD62L<sup>+</sup>) or effector memory CD4<sup>+</sup> T cells (CD44<sup>+</sup>CD62L<sup>-</sup>) on a dual laser FACS (Becton Dickinson) to more than 99% purity.

FACS analyses were performed on single-cell suspensions from cervical lymph nodes (cLNs), inguinal lymph nodes (iLNs), mesenteric lymph nodes (mLNs), Peyer patches (PPs), and spleen at indicated time points after HCT. For cell proliferation analysis splenocytes ( $1 \times 10^7$ /mL) were resuspended in plain phosphate-buffered saline (PBS) and stained with Vybrant CFDA SE (carboxyfluorescein diacetate, succinimidyl ester) Tracer kit (Molecular Probes, Eugene, OR) at a final concentration of 5 μM for exactly 6 minutes at 37°C. Immediately after staining, cells were washed in 5 volumes of ice-cold RPMI plus 10% fetal bovine serum (Gibco, Life Sciences, Grand Island, NY) twice, resuspended in PBS, and counted before intravenous injection. Flow cytometric data were analyzed with FlowJo Software (Treestar, Ashland, OR).

### Mixed leukocyte reaction

Unseparated splenocytes ( $10^5$ ) or fluorescence-sorted T-cell subsets from L2G85 FVB/N (H-2<sup>a</sup>) donor mice were used as responders and mixed with irradiated (3000 cGy) allogeneic Balb/c splenocytes (H-2<sup>d</sup>) as stimulators for MLRs. Responder-stimulator ratios were chosen to be 1:0, 1:1, and 1:4. Cultures were set up in triplicates in 96-well flat-bottom plates in a total volume of 200 μL. Cells were cultured in RPMI 1640 medium with 10% fetal calf serum (FCS), 10 mM HEPES (*N*-2-hydroxyethylpiperazine-*N'*-2-ethanesulfonic acid), 1% nonessential amino acids, 2 mM L-glutamine, 100 U/mL penicillin, 100 μg/mL streptomycin (all from GIBCO), and 5 μg/mL 2-mercaptoethanol (Sigma-Aldrich, St Louis, MO). Proliferation was assessed after 5 days by pulsing the cells with 0.037 MBq/well (1 μCi/well) [<sup>3</sup>H]thymidine (Amersham Biosciences, Freiburg, Germany) for the last 16 hours. Cells were harvested onto filter membranes using a Wallac harvester (Perkin-Elmer, Shelton, CT) and the amount of incorporated [<sup>3</sup>H]thymidine was measured with a Wallac Betaplate counter (Perkin-Elmer).

### Syngeneic and allogeneic HCT and in vivo imaging

To condition mice for HCT, a Phillips Unit Irradiator (250 kv, 15 milliamp) was used to deliver lethal radiation on day 0 relative to transplantation. Female 8- to 12-week-old HCT recipient mice received 2 split doses of either 400 cGy (allogeneic Balb/c recipients) or 450 cGy (syngeneic FVB/N recipients) 3 to 4 hours apart. For hematopoietic reconstitution, animals were injected with  $5 \times 10^6$  FVB/N wild-type BM cells intravenously within 3 hours after the second dose of radiation. To induce acute GVHD, wild-type mice were coinjected intravenously with FVB/N-L2G85 *luc*<sup>+</sup> splenocytes or with FACS sorted T-cell subpopulations from the spleen of 8- to 12-week-old female donors or 8- to 10-month-old donors, respectively. In vivo bioluminescence imaging (BLI) was performed as previously described, using an IVIS100 charge-coupled device (CCD) imaging system (Xenogen, Alameda, CA).<sup>8</sup>

### Ex vivo imaging and analysis

After in vivo BLI, mice were injected with an additional dose of luciferin (150 μg/g bodyweight, intraperitoneally). Five minutes later, animals were humanely killed. Selected tissues were prepared and imaged for 5 minutes. Tissue processing was timed to stay within a period of 3 minutes. Ex vivo BLI resulted in high-resolution images displaying signal foci within organs of interest and directed the embedding of tissues for histology as well as cell

extraction for FACS analysis. Imaging data were analyzed and quantified with Living Image Software (Xenogen) and Igor (WaveMetrics, Lake Oswego, OR).

### In vitro imaging of hematopoietic subpopulations

For analysis of luciferase expression in hematopoietic subsets, splenocytes were obtained from 8-week-old female *luc*<sup>+</sup> transgenic FVB/N mice. Cell populations were FACS sorted to more than 99% purity. Cells were placed into black flat-bottom 96-well tissue culture plates and incubated in complete RPMI (Gibco Lifetechnologies, plus 1% penicillin/streptomycin, 1% L-glutamine, 10% fetal calf serum, and 0.1% mercaptoethanol) for 12 hours. Prior to imaging, 2 μL of luciferin (30 mg/mL) were added into each well containing exactly  $1 \times 10^5$  cells in 200 μL media. After BLI, cells were reanalyzed by propidium iodide staining and flow cytometry to exclude dead cells from the calculation of light emission per cell.

### Immunofluorescence microscopy

Tissues were sampled over the time course of 6 days and cryopreserved at -80°C. Fresh frozen sections of 5 μm thickness were mounted on positively charged precleaned microscope slides (Superfrost/Plus; Fisher Scientific, Hampton, NH) and stored at -80°C. The sections were initially thawed for 20 minutes at room temperature (RT). After acetone fixation (7 minutes at RT) and air drying (3 minutes), sections were incubated with blocking solution (PBS + 2% FCS) for 15 minutes. Incubations with primary antibodies were performed for 1 hour at RT. Directly conjugated antibodies were used for lineage determination of T lymphocytes (CD8-FITC and CD4-PE; BD Pharmingen) diluted 1:200 in  $1 \times$  PBS. The donor T-cell marker Thy1.1-APC (BD Pharmingen) was used 1:100 in PBS. Nuclei were stained with DAPI (4',6-diamidino-2-phenylindole). Washing steps after antibody incubation and DAPI staining were performed in  $1 \times$  PBS (3 times, 3 minutes each). Fluorescence microscopic evaluation was performed on a Nikon microscope (Eclipse, TE 300; Melville, NY). Microscopic photos were obtained using a Spot digital camera (Diagnostic Instruments, Sterling Heights, MI). Digital images were saved as TIFF files and inserted and processed in PowerPoint (Microsoft Office, Redmond, WA). Standard magnifications were 200×/numerical aperture 0.45 and 400×/numerical aperture 0.60.

## Results

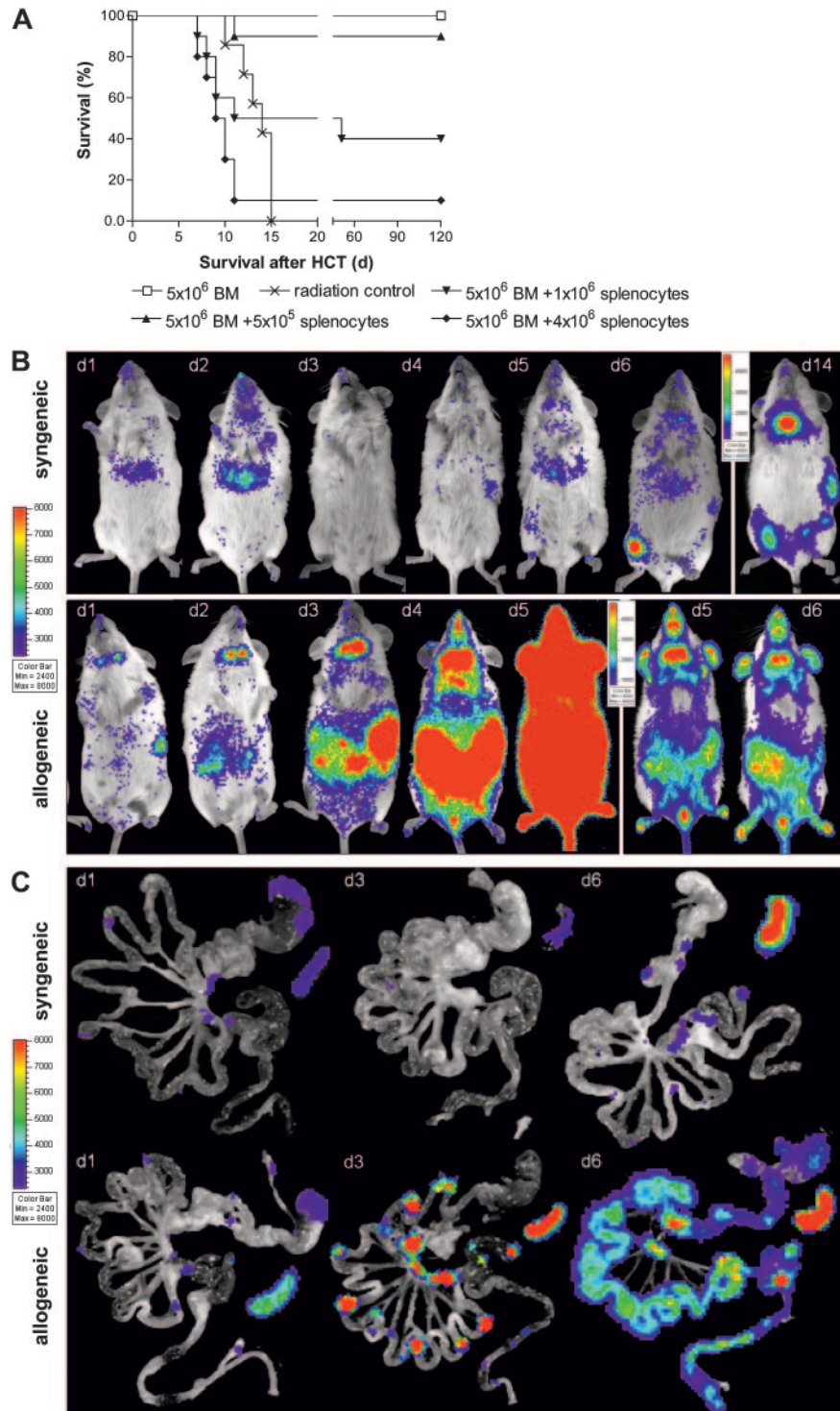
### Tracking *luc*<sup>+</sup> transgenic donor cells after HCT

To study proliferation and migration of unmanipulated donor cells in vivo, we used a luciferase (*luc*)–expressing transgenic donor mouse line (designated L2G85; FVB/N background). The transgene consisted of the chicken-β-actin promoter and a dual reporter gene, comprising the coding sequences for *luc* and enhanced green fluorescent protein (*eGFP*). Splenic T cells as well as other hematopoietic cells from L2G85 donors expressed luciferase; the level of light emission was similar for CD4<sup>+</sup> and CD8<sup>+</sup> T cells, and was highest for CD11b<sup>+</sup> populations.<sup>9</sup> *eGFP* was only detected in a few nonhematopoietic tissues such as skin and heart muscle of newborn L2G85 mice, but not in hematopoietic cell lineages.

To characterize the acute GVHD induction potential of FVB/N splenocytes (H-2<sup>a</sup>) in Balb/c recipients (H-2<sup>d</sup>), we performed mixed leukocyte reactions (MLRs). FVB/N splenocytes proliferated in a similar fashion to C57Bl/6 splenocytes against Balb/c stimulators. FVB-L2G85 *luc*<sup>+</sup> transgenic splenocytes were functionally comparable to FVB/N wild-type splenocytes (data not shown). MLR could also demonstrate that the *luc*<sup>+</sup> transgene was not recognized immunologically (data not shown).

To establish optimal study conditions for acute GVHD we performed HCT experiments in lethally irradiated Balb/c recipients receiving  $5 \times 10^6$  FVB/N bone marrow (BM) cells to re-establish

**Figure 1. Transplantation of transgenic luciferase<sup>+</sup> splenocytes.** (A) Transplantation of allogeneic FVB/N splenocytes induces acute lethal GVHD in a cell dose dependent manner. All animals that received transplants of  $5 \times 10^6$  allogeneic bone marrow cells ( $\square$ ;  $n = 10$ ) survive without GVHD, whereas mice receiving lethal irradiation (800 rad) without subsequent HCT die of the consequences of myeloablation ( $\times$ ;  $n = 7$ ). HCT recipients that received transplants of  $5 \times 10^6$  allogeneic bone marrow plus  $5 \times 10^5$  allogeneic splenocytes ( $\blacktriangle$ ;  $n = 10$ ), or plus  $1 \times 10^6$  allogeneic splenocytes ( $\blacktriangledown$ ;  $n = 10$ ) develop acute GVHD. Mice that received transplants of bone marrow plus  $4 \times 10^6$  allogeneic splenocytes die of lethal acute GVHD within 2 weeks after HCT ( $\blacklozenge$ ;  $n = 10$ ). Displayed are pooled results from 2 independent experiments. (B) BLI and (C) ex vivo imaging demonstrate a dynamic process of cell proliferation and migration with distinct distribution patterns in syngeneic versus allogeneic HCT recipients. Syngeneic splenocytes (top row) home initially predominantly to the liver and display signs of hematopoietic engraftment by day 6. By day 14, syngeneic HCT display predominant signals from the bone such as femura, pelvis, and sternum, but also spleen and thymus. Allogeneic transplanted splenocytes (bottom panel) initially proliferate in secondary lymphoid organs before infiltrating the intestines at day 4, liver and skin (ears) between day 5 and 6. Animals with an oversaturating light signal are displayed with increased signal thresholds to resolve the predominant organ distribution. One representative animal for each group is shown over time. Ex vivo imaging of the gastrointestinal tract and spleen of syngeneic animals (C, top row) reveals only transient migration of splenocytes to Peyer patches and mesenteric lymph nodes but an increase of light emission from the spleen. In contrast, allogeneic splenocytes (C, bottom row) migrate to and proliferate in these lymphoid organs before infiltrating mucosal sites. Signals from the entire intestines start to peak at day 6 before animals succumb to acute lethal GVHD.



hematopoiesis by intravenous injection. FVB/N bone marrow alone rescued all Balb/c recipients from irradiation-induced lethality, without signs of GVHD (Figure 1A). In contrast, addition of increasing numbers of FVB-L2G85 *luc*<sup>+</sup> splenocytes induced acute lethal GVHD in a dose-dependent manner. While most animals recovered following an injection of  $5 \times 10^5$  splenocytes, the majority of animals succumbed within 12 days following an injection of  $1 \times 10^6$  and  $4 \times 10^6$  splenocytes. The latter group of mice displayed all features of acute GVHD, including diarrhea, weight and hair loss, and hunched back. Since we aimed to

investigate the most severe course of acute lethal GVHD, we decided to use  $4 \times 10^6$  *luc*<sup>+</sup> splenocytes for subsequent experiments.

#### In vivo BLI shows temporal and spatial dynamics of acute GVHD

Allogeneic Balb/c recipients showed a dramatic BLI signal increase within the first 6 days after transfer of  $4 \times 10^6$  *luc*<sup>+</sup> splenocytes as measured by total body photon emission. BLI revealed signals from the abdominal region, the spleen, and the cervical lymph node area within 1 day after transfer (Figure 1B,

lower panel). The abdominal signals rapidly increased by day 3, to become intense and uniform by day 4. This abdominal increase preceded apparent infiltration of the skin, which occurred on days 5 and 6 as indicated by BLI signals from ears and paws. Indicative of massive cell proliferation, BLI signals were extremely intense by day 5 and changes in the camera settings were necessary to accommodate the intensity (threshold increase, Figure 1B, lower panel, days 5, 6).

To distinguish homeostatic cell proliferation and engraftment from acute GVHD we simultaneously transplanted *luc*<sup>+</sup> L2G85-FVB splenocytes plus wild-type FVB/N bone marrow cells into syngeneic recipients (FVB/N, wild type; Figure 1B, upper panel). BLI on syngeneic recipients showed waves of transient homing and proliferation over the liver in the first days after transplantation. The spleen showed weak BLI signals until day 5 after syngeneic transplantation. Starting on day 6 we observed signs of hematopoietic engraftment, predominantly in femora and pelvis and in the spleen (day 14), while distinct signals were also apparent over the thymus (day 14).

#### **Ex vivo BLI defines mLN, PP, and spleen as crucial sites of alloreactive expansion**

Due to dramatic signal increases over the abdomen of allogeneic recipients, we decided to investigate this compartment in greater detail. First, we established optimal conditions for ex vivo imaging of bioluminescent signals from freshly prepared organs, with a particular focus on the gastrointestinal tract (GIT). Subsequently, we humanely killed representative animals of each experimental group and prepared the GIT for ex vivo analyses (Figure 1C).

Within 12 hours after transplantation, ex vivo analyses of allogeneic GIT tissues revealed signals over Peyer patches (PPs) and mesenteric lymph nodes (mLNs; Figure 1C, lower panel). Furthermore, we observed transient BLI signals over gastric fundus<sup>13</sup> and perirectal LNs. By days 2 and 3 signals dramatically increased over PPs, mLNs, the celiac patch, and spleen. By day 6 the entire GIT showed strong and diffuse BLI positivity, including small bowel, large bowel, stomach, and esophagus of allogeneic recipients. These findings correlated well with the symptoms of acute gut GVHD.

Syngeneic GIT samples on day 1 showed weak BLI signals, similar in distribution and strength to allogeneic recipients at this early time point (Figure 1C, upper panel). In contrast, BLI signals on syngeneic recipients remained weak throughout the first 5 days after splenocyte transfer. The signals were indicative of transient infiltration of lymphoid organs without signs of active proliferation or signs of GVHD. Ex vivo analysis of the syngeneic spleen confirmed a BLI signal increase, indicative of either hematopoietic engraftment or homeostatic proliferation.

#### **Initial CD4<sup>+</sup> T-cell expansion in lymphatic organs shifts rapidly to CD8<sup>+</sup> response**

Due to the dramatic GIT involvement at early time points during acute GVHD we explored the infiltration of allogeneic donor T cells in greater detail. We used BLI to target sites for analysis by triple-color immunofluorescence. Fresh frozen sections were stained for CD4, CD8, and the donor-specific T-cell marker Thy1.1. PPs showed infiltration of CD4<sup>+</sup> donor T lymphocytes in parafollicular T zones as early as 12 hours after transfer (Figure 2A,E,I). Thy1.1<sup>+</sup> donor T cells were not found in subepithelial dome regions (SEDs) or B-cell follicles of PPs at this early time point (12 hours after transfer). Similarly, donor T cells showed specific homing within

12 hours to the subcortical T zones of cLNs, mLNs, and periaarteriolar lymphoid sheaths (PALs) of the spleen (data not shown). By day 3 a significant increase in BLI signals of PPs, mLNs, and the spleen was observed, suggesting proliferation (Figure 2B). Histological examination revealed that PPs were beginning to collapse and were infiltrated primarily by CD4<sup>+</sup> donor T cells (Figure 2F,J). By day 4 BLI signals spread out into adjacent areas of PPs to become confluent in the aboral parts of the small bowel (ileum and jejunum; Figure 2C). A dense infiltration of donor-derived CD4<sup>+</sup> T cells could now be observed in the PPs (Figure 2G,K). By day 6 complete infiltration of the small and large bowel was apparent (Figure 2D). By this time the PPs had collapsed and were now mainly infiltrated by donor CD8<sup>+</sup> cells, which had also diffusely infiltrated the entire intestinal mucosa (Figure 2H,L).

We did not observe donor B-cell infiltration (CD19<sup>+</sup>, H-2k<sup>q</sup>) in PPs at any of the analyzed time points. Most PP follicles instead demonstrated radiation-induced necrosis at early time points (12, 24, and 48 hours), surrounded by foamy macrophages, which showed a high degree of autofluorescence (either cytoplasmic, or as amorphous and anuclear signals), particularly in the green color channel (Figure 2I-L).

mLNs, spleen, and small bowel were also analyzed at days 3, 4, and 6 after HCT (Figure 3). On day 3, predominantly CD4<sup>+</sup> donor lymphocytes were observed in mLNs, spleen (Figure 3A,E), while the small bowel was still negative for donor T cells (Figure 3I). By day 4 infiltration of donor CD8<sup>+</sup> T cells became more predominant in mLNs and spleen, while the intestinal mucosa now showed infiltration by CD4<sup>+</sup> donor T cells (Figure 3B,F,J).

We furthermore observed donor-cell infiltration also in other target organs of allogeneic recipients, such as skin, liver, and colon. By day 6 these infiltrates consisted of both donor-derived CD4<sup>+</sup> and CD8<sup>+</sup> T cells, which were often found in direct cellular contact (Figure 3M,N,O).

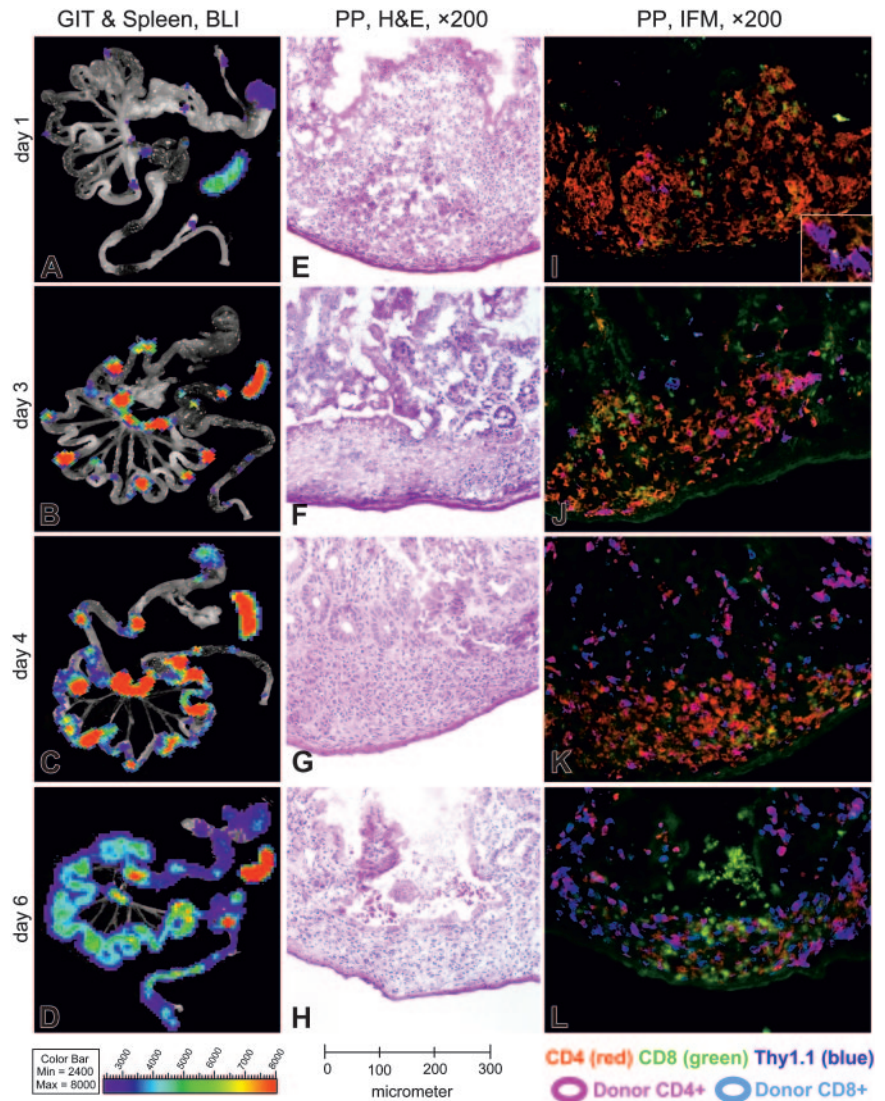
Control tissues of mice, which received only lethal irradiation 6 days prior to sampling, stained negative for the donor marker Thy1.1. Interestingly, PPs were the only site where CD4<sup>+</sup> host T cells seemed to survive until day 6 (Figure 3P). In contrast only few weakly stained CD4<sup>+</sup> host cells were found in mLNs, spleen, and intestinal tissues at this time point (Figure 3D,H,L).

To gain further insight into the composition of the cellular infiltrates of PPs, mLNs, spleen, and small intestines, we counted the number of donor CD4<sup>+</sup> and CD8<sup>+</sup> T cells per microscopic high-power field ( $\times 400$ ). In all tissues CD4<sup>+</sup> T cells preceded CD8<sup>+</sup> T-cell infiltration (Figure 4A). The spleen was the first lymphatic organ to show a shift in favor of the CD8<sup>+</sup> donor population, resulting in a CD4/CD8 ratio of 1:1.5 on day 4. The mLNs displayed a similar shift on day 5 equaling a CD4/CD8 ratio of 1:1.8.

#### **Donor T cells expressing the gut-homing receptor $\alpha 4\beta 7$ integrin arise from distinct lymphoid organs**

To study phenotypic changes of infiltrating donor T cells we characterized the expression of activation markers such as CD25, CD44, and CD69 on donor CD4<sup>+</sup> and CD8<sup>+</sup> T cells. We used FACS to analyze donor-cell infiltrates in spleen, cLNs, mLNs, iLNs and PPs of animals that received transplants at specific time points (Figure 4B). Only few donor cells were identified at the earliest time point after intravenous injection (12 hours). Analysis of samples from day 3 in contrast showed an appreciable number of donor CD4<sup>+</sup> and CD8<sup>+</sup> T cells, of which approximately 70% to 80% expressed the activation marker CD44. By day 6 more than 93% of the donor T cells were CD44<sup>+</sup>. CD69 expression in contrast

**Figure 2. BLI of gastrointestinal tissues and spleen combined with histology and immunofluorescence microscopy of Peyer patches during induction of acute GVHD.** (A-D) Until day 3 after allogeneic HCT, BLI signals increase over Peyer patches (PPs), mesenteric lymph nodes (mLNs) and the spleen, while staying confined to these organs. Day 4 represents a transition, showing spread of BLI signals within the small bowel, preferentially in areas adjacent to PPs. Day 6 shows a diffuse BLI signal, covering the entire GIT. BLI signal increased over the spleen until day 3 and remained highly positive until day 6. (E-H) In H&E staining, the PPs of day 1 show irradiation-induced necrosis of B-cell follicles surrounded by large macrophages loaded with nuclear debris, which showed a high degree of green autofluorescence (compare panels I-L). Between days 3 and 4 the B-cell follicles disappear completely and are replaced by histiocytic infiltrates, while the T-cell zones appear to be conserved. On day 6 the architecture of PPs is further disturbed by a collapse of dome regions, leaving behind a flat structure, diffusely infiltrated by lymphocytes. (I-L) Triple-color staining performed with CD4-PE (red), CD8-FITC (green), and Thy1.1-APC as donor-specific marker (blue). CD4<sup>+</sup> donor T cells specifically home to parafollicular T-cell areas of PPs within 1 day after transfer of splenocytes, while completely sparing subepithelial dome regions and B-cell follicles. Donor-derived CD4<sup>+</sup> T cells clearly dominate in PPs over CD8<sup>+</sup> T cells until day 3 and stay confined to the T-cell areas. The transition on day 4 shows a diffuse emigration of donor T cells, which become visible in the small bowel mucosa and submucosa adjacent to the PPs. On day 6 the PPs and other parts of the intestine are diffusely infiltrated by donor T cells, now predominantly CD8<sup>+</sup>.



followed a different time course, showing highest expression (approximately 25%) on day 3, while gradually declining on day 4 and 6. These changes of activation markers on donor T cells were comparable between PPs, mLNs, cLNs, and spleen.

We also evaluated expression of the homing receptors  $\alpha 4\beta 7$  integrin and L-selectin (CD62L; Figure 4B, bottom panels).<sup>14-16</sup> In the spleen donor, CD4<sup>+</sup> T cells mostly expressed CD62L but not  $\alpha 4\beta 7$  at early time points (12 hours and 3 days), whereas a significant proportion of donor-derived CD8<sup>+</sup> T cells expressed both  $\alpha 4\beta 7$  and CD62L (12 hours). Over time CD62L expression was lost, while  $\alpha 4\beta 7$  became up-regulated. As shown by BLI and confirmed by histology, day 3 was the latest time point that alloreactive donor T cells were confined to lymphoid organs before infiltrating mucosal GVHD target sites. Therefore, detailed analysis of  $\alpha 4\beta 7$  expression on donor CD4<sup>+</sup> and CD8<sup>+</sup> T cells in different tissues was performed on day 3, since this time point appeared to be critical to the activation and homing of alloreactive T cells. Within PPs and mLNs a significant number of donor CD4<sup>+</sup> and CD8<sup>+</sup> T cells up-regulated the gut-homing receptor  $\alpha 4\beta 7$  (Figure 4C). This stood in contrast to cLNs, in which only very few  $\alpha 4\beta 7$ <sup>+</sup> cells were detected. We also found significant numbers of  $\alpha 4\beta 7$ <sup>+</sup> donor CD8<sup>+</sup> T cells in the spleen. On day 6,  $\alpha 4\beta 7$ <sup>+</sup> donor T cells of CD4<sup>+</sup> and CD8<sup>+</sup> origin were observed in all lymphoid

tissues (data not shown). Interestingly, we observed a link between proliferation stage and up-regulation of homing molecules, as demonstrated by CFSE (carboxyfluorescein succinimidyl ester) analysis (Figure 4D). Before, or possibly during the first cell cycle, donor CD4<sup>+</sup> and CD8<sup>+</sup> T cells down-regulated  $\alpha 4\beta 7$ . After a phase of slow and modest up-regulation between generations 2 and 5,  $\alpha 4\beta 7$  integrin became highly up-regulated after the sixth cell division. This phenomenon was most pronounced in donor T cells derived from the mLNs (Figure 4D).

In summary, ex vivo imaging, histology, and FACS analysis revealed the initiation of GVHD in secondary lymphoid organs. Gut-homing alloreactive T cells were shown to develop specifically in Peyer patches, mLNs, and spleen, but not in peripheral lymphoid organs such as cLNs and iLNs.

#### Trafficking of naive and effector memory CD4<sup>+</sup> T cells

As described under "Initial CD4<sup>+</sup> T-cell expansion in lymphatic organs shifts rapidly to CD8<sup>+</sup> response," above, the combination of CD4<sup>+</sup> and CD8<sup>+</sup> T lymphocytes contained in the transplanted splenocytes induced acute GVHD. Furthermore, FACS-sorted CD4<sup>+</sup> or CD8<sup>+</sup> T cells transplanted separately both caused acute lethal GVHD (data not shown). Since GVHD initiation took place exclusively in secondary lymphoid organs, we wanted to test whether T-cell subsets incapable of

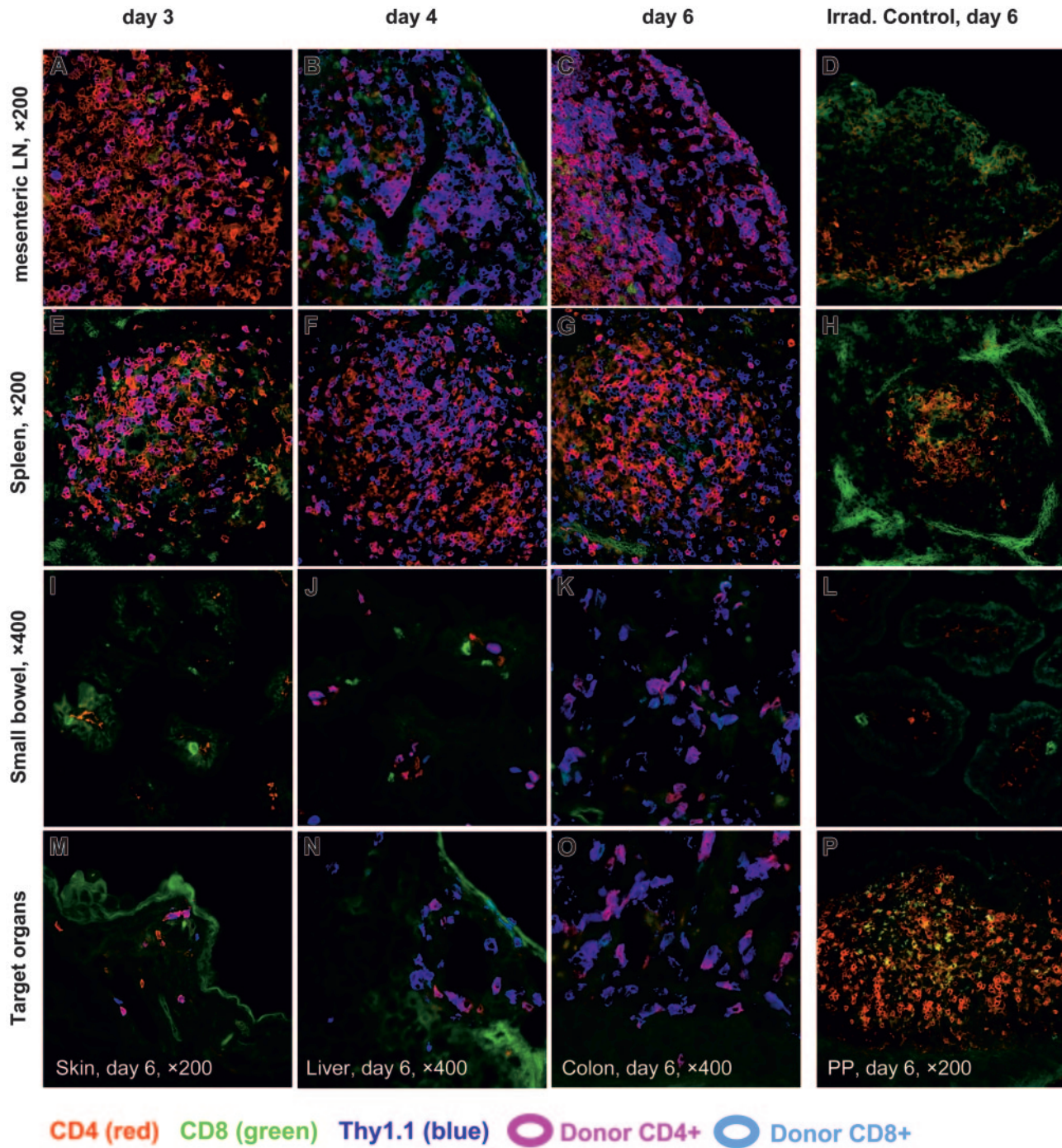


**Figure 3. Triple-color immunofluorescence microscopy (IFM) of secondary lymphatic tissues and GVHD target organs.** IFM was performed using 3 T-lymphocyte markers (antibody-conjugates): CD4-PE (red), CD8-FITC (green), and the donor-specific T-cell marker Thy1.1-APC (blue). Fresh frozen tissues sampled on 3 time points after transfer of allogeneic splenocytes (3, 4, and 6 days) are shown for mesenteric lymph nodes (mLNs) (panels A-C), spleen (panels E-G), and small bowel (panels I-K). Lymphatic tissues of day 3 (panels A,E) display a predominant infiltration by CD4<sup>+</sup> donor T cells, which are confined to the corresponding T zones of mLNs and spleen, while target organs of day 3 remain negative for donor T cells. Day 4 represents a dramatic change in that the small bowel mucosa as a GVHD target tissue (panel J) is now infiltrated by donor T lymphocytes, predominantly CD4<sup>+</sup>, while lymphatic organs (panels B,F) shift to an expansion of CD8<sup>+</sup> donor T cells (compare also Figure 4A). On day 6 all relevant GVHD target tissues are infiltrated by donor T cells, now predominantly CD8<sup>+</sup>, which are frequently in contact with CD4<sup>+</sup> T cells of donor origin and sporadically with host CD4<sup>+</sup> T cells (panels K,M-O). CD4<sup>+</sup> and CD8<sup>+</sup> T cells of host origin have mostly disappeared in mLNs, spleen, and small bowel of control tissues of Balb/c mice on day 6 after irradiation, which had not received an allogeneic transplantation (panels D,H,L). In contrast, PP samples of this control mouse show numerous CD4<sup>+</sup> host T cells, which display a distinct membrane staining (panel P). The costaining for Thy1.1 was negative on all of the control tissues.

entering these sites would cause GVHD. T<sub>EM</sub> cells are a heterogeneous cell population characterized by several surface markers.<sup>17,18</sup> A common denominator of T<sub>EM</sub> cells is the lack of homing receptors such as L-selectin and chemokine receptor 7 (CCR7), which are found on naive T cells and allow for migration from the bloodstream into T-cell zones of lymph nodes and Peyer patches.<sup>19-21</sup> The aim was to compare T<sub>EM</sub> cells

with purified naive T cells regarding their migration pattern and their potential to cause GVHD. We FACS sorted triplicates of 10<sup>5</sup> *luc*<sup>+</sup> naive T cells (CD4<sup>+</sup> CD44<sup>-</sup> CD62L<sup>+</sup>) and T<sub>EM</sub> cells (CD4<sup>+</sup> CD44<sup>+</sup> CD62L<sup>-</sup>) into 96-well plates (Figure 5A). BLI revealed that FACS-sorted *luc*<sup>+</sup> T<sub>EM</sub> cells emitted 3-fold more photons/cell/second than naive T cells (Figure 5B).

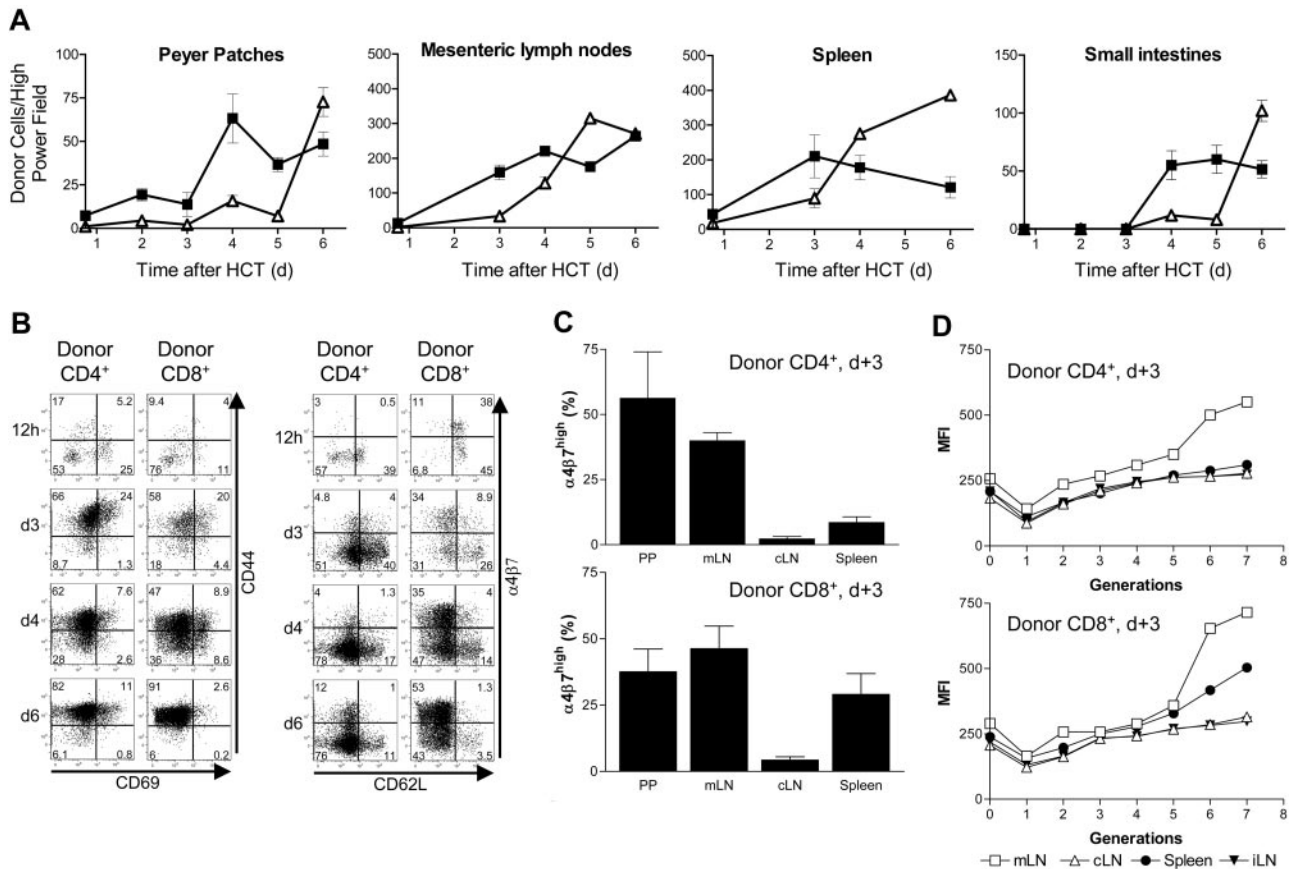


**Figure 4. Evaluation of infiltrating donor-derived T cells in allogeneic target tissues.** (A) Allogeneic CD4<sup>+</sup> T cells precede the increase of donor CD8<sup>+</sup> T cells in lymphoid organs during GVHD initiation. Shown are absolute numbers of donor-derived T cells in high-power fields (HPFs) by IFM. The shift from donor CD4<sup>+</sup> (■) to CD8<sup>+</sup> T cells (Δ) occurred first in the spleen on day 4 and later in other lymphoid organs. Donor CD4<sup>+</sup> T cells appear in the small intestines after extensive proliferation in lymphoid organs not earlier than day 4 after HCT followed by infiltrating cytotoxic T cells (Standard deviation was calculated using cell counts from 3 to 4 HPFs of 2 experimental mice for each time point). (B) FACS analysis of donor (H-2K<sup>b</sup>) lymphocytes reveals changes in expression profiles of activation and homing markers. The up-regulation of CD69 in donor CD4<sup>+</sup> and CD8<sup>+</sup> T cells is followed by CD44 expression. Up-regulation of α4β7 differs between donor CD4<sup>+</sup> and CD8<sup>+</sup> T cells in the spleen. Shown is a representative experiment (of 2-3 independent experiments) in which cells were pooled from the spleens of allogeneic transplant recipients (n = 3-5/time point). The numbers in each quadrant represent percentages of cells. (C) Donor CD4<sup>+</sup> T cells with gut-homing potential appear in PPs and mLNs until day 3 after HCT before donor CD4<sup>+</sup> T cells start to appear in mucosal sites of the intestines. On day 3 after HCT the frequency of α4β7<sup>hi</sup> donor CD4<sup>+</sup> T cells in PPs and mLNs is significantly higher in cells primed in vivo by PPs and mLNs versus spleen and cLNs. α4β7<sup>hi</sup> donor CD8<sup>+</sup> T cells can be found in the spleen in addition to PPs and mLNs, but only a few are found in cLNs. Error bars indicate the standard deviation of 3 independent experiments. (D) CFSE proliferation analysis demonstrated that it takes more than 5 cell divisions before up-regulation of α4β7 integrin occurred in mLNs (> 98% of all α4β7<sup>hi</sup>). Peripheral LNs such as cLNs and iLNs do not contain gut-homing T cells. (PPs are not shown because of too-low cell yields for CFSE analysis.)

Young donor mice (8-10 weeks) that are kept in a laboratory setting have a rather small T<sub>EM</sub>-cell pool, while the naive T-cell pool is large. It is known that naive T cells have a highly diverse T-cell receptor repertoire.<sup>17</sup> If a diverse T-cell repertoire is more likely to contain alloreactive T-cell clones, the size of this T-cell pool becomes of high importance. To this end we performed mixed leukocyte reactions in which we compared proliferation of FACS-sorted naive T cells versus T<sub>EM</sub> cells derived from either young donors (8-10 weeks of age) or aged donors (8-10 months; Figure 5C). Naive allogeneic T cells (CD4<sup>+</sup>) from young and aged donors proliferated in this MLR at a comparable level to whole splenocytes. Of importance, T<sub>EM</sub> cells from aged donors were highly alloreactive in these MLRs, in contrast to T<sub>EM</sub> cells from young donors.

It remained to be tested whether both T-cell subsets would be capable of inducing GVHD in vivo. Therefore, we transplanted 5 × 10<sup>5</sup> sorted CD4<sup>+</sup> naive T cells versus T<sub>EM</sub> cells (purity > 99%) from luc<sup>+</sup> transgenic FVB/N donors together with 5 × 10<sup>6</sup> wild-type bone marrow cells. Mice given transplants of naive T cells died of acute GVHD within 40 to 60 days in contrast to a 100% survival in mice that received the same number of T<sub>EM</sub> cells from aged donors (Figure 5D). Despite the strong in vitro proliferation,

T<sub>EM</sub> cells from aged donors did not cause GVHD (Figure 5D-E). Naive T cells showed homing to PPs, mLNs, and spleen followed by a rapid expansion, comparable to BLI patterns observed after whole splenocyte transfer (Figure 5E). In contrast, T<sub>EM</sub> cells from aged donors showed only transient homing to liver and nose-associated lymphatic tissues (NALTs) with limited T<sub>EM</sub> cell expansion in allogeneic recipients (Figure 5E).

Histomorphologic evaluation of liver samples confirmed a severe graft-versus-host reaction on the bile ducts of mice that had received CD4<sup>+</sup> naive T lymphocytes from aged donors 6 days prior, equaling a grade IV GVHD.<sup>22-24</sup> We observed a widespread loss of bile duct epithelia (> 80%) in these animals (Figure 5F, arrow), accompanied by a diffuse infiltration of lymphocytes in the portal triads. Furthermore, hepatocytes in these animals showed fatty changes and hydropic degeneration as potential signs of inflammation and metabolic stress. In contrast, liver samples of mice that had received allogeneic CD4<sup>+</sup> T<sub>EM</sub> cells from aged donors 6 days prior displayed intact bile ducts with regular epithelia without apoptosis (Figure 5G, arrow). We did not find any signs of inflammation within the portal triads of these mice, while hepatocytes looked normal throughout the observation period. Rarely, we found single lymphocytes in perivascular regions.

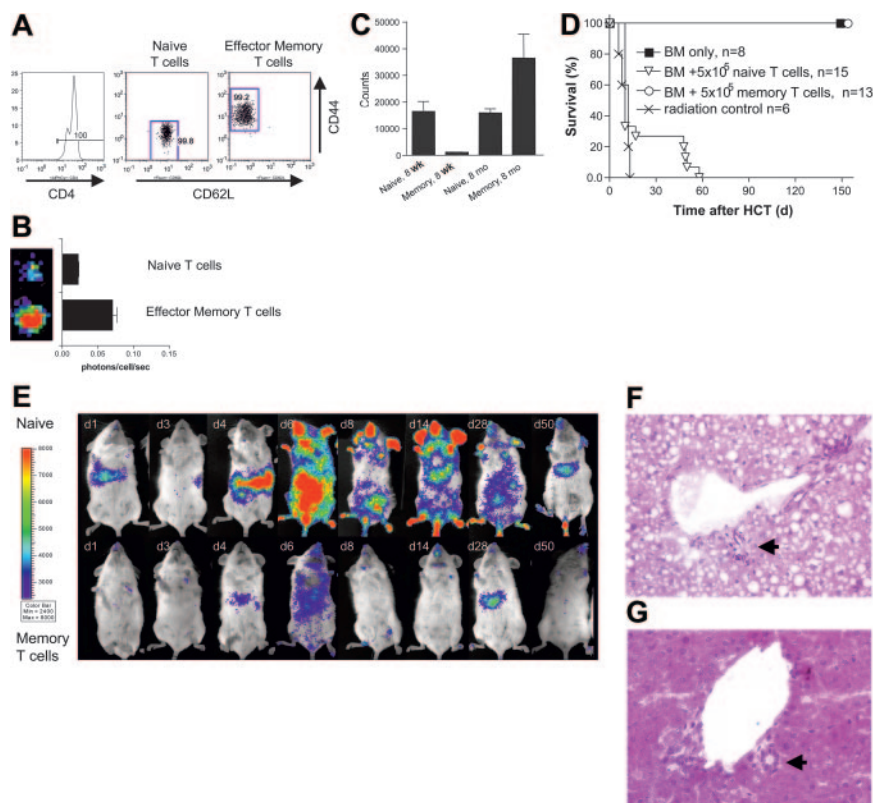


**Figure 5. Allogeneic CD4<sup>+</sup> T<sub>EM</sub> cells of aged mice are highly alloreactive in vitro without causing GVHD in vivo.** (A) MACS-enriched CD4<sup>+</sup> T cells (FVB/N-L2G85, H-2<sup>d</sup>) were sorted upon the expression of CD44<sup>lo</sup>CD62L<sup>hi</sup> (naive CD4<sup>+</sup> T cells) and CD44<sup>hi</sup>CD62L<sup>lo</sup> (effector memory CD4<sup>+</sup> T cells [T<sub>EM</sub>]) and transplanted with  $5 \times 10^6$  FVB/N wild-type bone marrow cells into lethally irradiated Balb/c recipients (H-2<sup>d</sup>). Cell purity of these populations exceeded more than 99% (numbers on plots represent percentages of cells). (B) Naive CD4<sup>+</sup> T cells emit less light than CD4<sup>+</sup> T<sub>EM</sub> cells.  $10^5$  CD4<sup>+</sup> T-cell subsets were FACS sorted and bioluminescence quantified (error bars indicate SD of triplicates). (C) FACS-sorted CD4<sup>+</sup> T<sub>EM</sub> cells of old donor animals showed a strong alloreactive response to irradiated splenocytes in MLR experiments ( $10^5$  sorted T<sub>EM</sub> cells from 8-month-old FVB/N donors against Balb/c). Interestingly, CD4<sup>+</sup> T<sub>EM</sub> cells of young donor mice (8 weeks old) did not show an alloresponse in vitro. In contrast, naive CD4<sup>+</sup> T cells were alloreactive in this MLR independent of age of the donor (8-10 weeks vs 8-10 months). The bars represent the means of triplicate values and the brackets indicate SDs. One of 3 experiments with similar results is shown. (D) All allogeneic recipients of transplants of either bone marrow cells alone or bone marrow cells plus CD4<sup>+</sup> T<sub>EM</sub> cells of 8-month-old donors survived and performed well without any signs of GVHD until the end of the observation period. Animals that received allogeneic naive CD4<sup>+</sup> T cells and bone marrow all died of acute GVHD, either within 14 days or between days 40 to 60 after HCT. (E) Naive CD4<sup>+</sup> T cells of 8-month-old donor mice displayed similar proliferation and migration patterns as animals given transplants of whole splenocytes. Early gut infiltration is correlated with severe acute GVHD and early mortality. Although mice that survived more than 2 weeks after HCT show a decrease of the abdominal BLI signal, they displayed clinical signs of GVHD and persistent *luc*<sup>+</sup> T cells in liver and skin measured by BLI. One representative animal is shown from the latter category surviving until day 55. Allogeneic CD4<sup>+</sup> T<sub>EM</sub> cells undergo only a very limited cell proliferation phase until day 6 and home preferentially to the liver. (F) Liver sample of an animal that had received naive CD4<sup>+</sup> T lymphocytes (day 6 after transfer) showed severe damage of the bile duct epithelia (arrow), indicative of grade IV GVHD of the liver. Dispersed in periductular and perivascular regions of portal triads, lymphocyte infiltration was observed (compare Figure 3N). In addition, the liver samples of this group showed mixed fatty changes of hepatocytes and hydropic degeneration. (G) Liver samples of mice that had received allogeneic CD4<sup>+</sup> T<sub>EM</sub> cells of 8-month-old donors displayed intact bile ducts with a regular epithelial lining (arrow). No signs of inflammation were detected and hepatocytes looked normal, while only single lymphocytes were visible in perivascular regions. Images in panels F and G show hematoxylin-eosin stains at 200 $\times$  magnification.

Taken together, naive T cells caused GVHD that was initiated in secondary lymphoid organs and followed by GVHD manifestation in target organs such as gut, liver, and skin. In contrast, transplanted CD4<sup>+</sup> T<sub>EM</sub> cells did not proliferate in secondary lymphoid organs in vivo and despite their alloreactivity in vitro did not cause acute GVHD.

## Discussion

Clinical GVHD in murine and human recipients displays remarkable tissue tropism involving primarily gut, liver, and skin.<sup>6</sup> The recognition of either major or minor histocompatibility antigens followed by cellular proliferation in lymphoid organs and infiltration of GVHD target organs results in serious tissue damage. In vivo BLI allowed a comprehensive visualization of cell migration and expansion in vivo, including the infiltration of GVHD target

tissues. Ex vivo BLI enabled an even more precise localization of cellular infiltrates, which allowed specific sampling of BLI-positive tissues for histology and FACS analyses. For example, PPs, which had vanished macroscopically as a consequence of irradiation, suddenly became accessible to further analysis because of BLI-guided tissue sampling.

Analyses of lymphoid organs at early time points clearly demonstrated that expansion of CD4<sup>+</sup> T cells preceded CD8<sup>+</sup> T cells. Allogeneic T-cell activation occurred in several lymphoid organs. After initial down-regulation of CD62L, the gut-homing receptor  $\alpha 4\beta 7$  integrin was up-regulated only on donor T cells in PPs, mLNs, and spleen. Occurrence of  $\alpha 4\beta 7^{\text{hi}}$  T cells in the spleen during GVHD onset was recently described.<sup>16</sup> In the spleen and in peripheral LNs  $\alpha 4\beta 7^{\text{hi}}$  CD4<sup>+</sup> cells represented only a small fraction. It is possible, that  $\alpha 4\beta 7^{\text{hi}}$  CD4<sup>+</sup> T cells were in transition through the spleen, since we did not see a dramatic increase of  $\alpha 4\beta 7^{\text{hi}}$  CD4<sup>+</sup> T cells. In contrast, the increase of  $\alpha 4\beta 7^{\text{hi}}$  CD8<sup>+</sup> T

cells from day 1 to day 6 could indicate active proliferation in the spleen itself. Interestingly, the peak of  $\alpha 4\beta 7^{\text{hi}}$  CD8<sup>+</sup> T cells in the spleen coincides with the onset of GIT infiltration by CD8<sup>+</sup> T cells between days 5 and 6. In GVHD target organs we observed direct cell contacts between CD4<sup>+</sup> and CD8<sup>+</sup> donor T cells at this time, which were suggestive of cellular interactions and potential synergisms. Nevertheless, separate transplantation of purified CD4<sup>+</sup> and CD8<sup>+</sup> T-cell populations into Balb/c recipients both induced lethal acute GVHD. Thus, donor CD8<sup>+</sup> T-cell function was not dependent on donor CD4<sup>+</sup> T cells.

A prior study has suggested a critical role for PPs in GVHD induction in animals receiving either no or sublethal irradiation.<sup>25</sup> Early infiltration of PPs was clearly demonstrated in our study, resulting in activation of donor-derived T cells; however, this function was not exclusively observed in PPs as T-cell activation was also observed in other sites. Alloreactive gut-homing T cells did not arise in PPs only but were also found in large numbers in mLNs and spleen. However, peripheral lymph nodes such as iLNs and cLNs did not show the potential to prime donor T cells for alloreactive gut homing within the critical first 3 days of GVHD initiation. This is in accordance with findings of other groups that used T-cell receptor (TCR) transgenic mouse models in vitro and in vivo.<sup>26-29</sup>

An intravital microscopy study recently described that in addition to secondary lymphoid structures and classical GVHD target organs, nonclassical organs as kidneys, connective tissues, and brain were infiltrated by *gfp*<sup>+</sup> donor cells.<sup>30</sup> In our study we did not find any bioluminescent signals in the kidneys or the brain during the entire observation period (up to 3 months). On the level of immunofluorescence microscopy, the kidneys were completely negative for donor-derived T lymphocytes. The only positive tissue in the head was found to be the NALT system. We never observed signals derived from the central nervous system itself. Furthermore, connective tissues were also completely negative for donor T cells on immunofluorescence microscopy and bioluminescence level.

Previous studies reported that memory T cells do not induce acute lethal GVHD, in contrast to naive T cells.<sup>10-12</sup> These observations were reported as comparable between minor and major mismatch transplantation models. Furthermore, memory T cells were shown to have functional graft-versus-tumor activity besides a variety of other immunologic functions.<sup>10-12</sup> In the present study we evaluated the trafficking and proliferation patterns of CD4<sup>+</sup> naive versus T<sub>EM</sub> cells in vivo. A likely explanation for the incapacity of T<sub>EM</sub> cells to induce GVHD could be their distinct trafficking patterns. Strikingly, both naive and T<sub>EM</sub> cells are potentially alloreactive in vitro. Of note, only T<sub>EM</sub> cells from aged donors but not from 8- to 10-week-old mice, the standard age group used in most GVHD studies,<sup>11</sup> were alloresponsive in the MLRs. Interestingly there was no difference in the naive T cells from young or old donors concerning their in vitro alloreactivity. It is conceivable that human T<sub>EM</sub> cells are more diverse than T<sub>EM</sub> cells of young mice kept in a laboratory setting. Foster and colleagues described in a recent paper that freshly sorted human memory T

cells would be less alloreactive in vitro than naive T cells.<sup>31</sup> They described a statistically significant difference in proliferation comparing human naive CD4<sup>+</sup> T cells to CD4<sup>+</sup> T<sub>EM</sub> cells in MLR.<sup>31</sup> However, their data show that CD4<sup>+</sup> T<sub>EM</sub> cells do proliferate strongly upon in vitro allorecognition. In this light our MLR findings of alloreactive proliferation of CD4<sup>+</sup> T<sub>EM</sub> cells of aged animals are correlating well with their human data.

Furthermore, we found that the absolute number of T<sub>EM</sub> cells in the spleen increased with the age of the donor animals (A.B., S.S., R.S.N., unpublished data). Friedman et al<sup>32</sup> observed less GVHD when transplanting splenocytes from aged donors. A shift from naive T cells toward T<sub>EM</sub> cells in aged mice could explain their findings.

As a functional explanation for acute GVHD initiation, it seems very likely that access to secondary lymphoid organs is of critical importance. Naive CD4<sup>+</sup> T cells fulfill this property in contrast to T<sub>EM</sub> cells. Indirect evidence about the importance of lymphoid organs comes from studies demonstrating retainment of alloresponsive T cells to lymphoid organs during the initiation phase of GVHD.<sup>33</sup> In contrast, nonalloreactive donor cells had been found in the circulation soon after transplantation. Another important finding was described by Shlomchik and colleagues, who showed the capacity of host APCs to induce GVHD.<sup>34</sup> Murai and colleagues described that blocking the access to PPs could inhibit acute GVHD.<sup>25</sup> In this context our study highlights the importance for donor T cells to access secondary lymphoid organs to initiate GVHD, and gives further insights into the kinetics and timing of this process.

Other populations of CD4<sup>+</sup> T cells which coexpress CD25 (T<sub>reg</sub>) cells have been shown by a number of groups, including our own, to suppress GVHD while not eliminating graft-versus-tumor responses.<sup>8</sup> Interestingly, only the CD62L<sup>+</sup> subpopulation of T<sub>regs</sub> were capable of suppressing GVHD in vivo, whereas both CD62L<sup>+</sup> and CD62L<sup>-</sup> T<sub>regs</sub> were capable of suppressing alloreactive T-cell proliferation in vitro.<sup>35,36</sup> Therefore, it appears that regulatory cells need to access lymphoid organs to suppress GVHD. On the other hand, T<sub>EM</sub> cells are alloreactive in vitro, but do not proliferate in lymphoid organs in vivo and do not cause GVHD. Patients could potentially benefit from a cotransfer of T<sub>EM</sub> cells because of enhanced bone marrow engraftment, improved immune reconstitution, and possible increased graft-versus-tumor reaction without GVHD risk.

The present study advances the understanding of T-lymphocyte behavior after allogeneic HCT by characterizing in detail the trafficking patterns of T-cell subsets in vivo. Definition of the trafficking capacities of T-cell subsets will help to refine immune reconstitution therapies by avoiding the risk of GVHD and help to improve outcomes following allogeneic transplantation.

## Acknowledgments

The authors would like to thank S. Burns-Guydish, T. Doyle, J. A. Olson, and R. T. Stovel for helpful comments and technical assistance.

## References

- Harrowitz M. Uses and growth of hematopoietic cell transplantation. In: Thomas ED, Blume KG, Forman SJ, Appelbaum FR, eds. *Thomas' Hematopoietic Cell Transplantation*. Malden, MA: Blackwell; 2004:9-15.
- Appelbaum FR. Haematopoietic cell transplantation as immunotherapy. *Nature*. 2001;411:385-389.
- Shizuru JA. The experimental basis for hematopoietic cell transplantation for autoimmune diseases. In: Thomas ED, Blume KG, Forman SJ, Appelbaum FR, eds. *Thomas' Hematopoietic Cell Transplantation*. Malden, MA: Blackwell; 2004:324-343.
- Sykes M, Sachs DH. Mixed chimerism. *Philos Trans R Soc Lond B Biol Sci*. 2001;356:707-726.
- Ferrara JL, Deeg HJ, Division of Pediatric Oncology D-FCIBMA. Graft-versus-host disease. *N Engl J Med*. 1991;324:667-674.
- Hill GR, Ferrara JL. The primacy of the gastrointestinal tract as a target organ of acute graft-versus-host disease: rationale for the use of cytokine shields in allogeneic bone marrow transplantation. *Blood*. 2000;95:2754-2759.

7. Edinger M, Cao YA, Vermeris MR, Bachmann MH, Contag CH, Negrin RS. Revealing lymphoma growth and the efficacy of immune cell therapies using in vivo bioluminescence imaging. *Blood*. 2003;101:640-648.
8. Edinger M, Hoffmann P, Ermann J, et al. CD4+CD25+ regulatory T cells preserve graft-versus-tumor activity while inhibiting graft-versus-host disease after bone marrow transplantation. *Nat Med*. 2003;9:1144-1150.
9. Cao YA, Wagers AJ, Beilhack A, et al. Shifting foci of hematopoiesis during reconstitution from single stem cells. *Proc Natl Acad Sci U S A*. 2004;101:221-226.
10. Anderson BE, McNiff J, Yan J, et al. Memory CD4+ T cells do not induce graft-versus-host disease. *J Clin Invest*. 2003;112:101-108.
11. Chen BJ, Cui X, Sempowski GD, Liu C, Chao NJ. Transfer of allogeneic CD62L- memory T cells without graft-versus-host disease. *Blood*. 2004;103:1534-1541.
12. Zhang Y, Joe G, Zhu J, et al. Dendritic cell-activated CD44<sup>hi</sup>CD8+ T cells are defective in mediating acute graft-versus-host disease but retain graft-versus-leukemia activity. *Blood*. 2004;103:3970-3978.
13. Sale GE, Farr A, Hamilton BL. The murine forestomach: a sensitive site for graft-versus-host disease. *Bone Marrow Transplant*. 1991;7:263-267.
14. Gallatin WM, Weissman IL, Butcher EC. A cell-surface molecule involved in organ-specific homing of lymphocytes. *Nature*. 1983;304:30-34.
15. Hamann A, Andrew DP, Jablonski-Westrich D, Holzmann B, Butcher EC. Role of alpha 4-integrins in lymphocyte homing to mucosal tissues in vivo. *J Immunol*. 1994;152:3282-3293.
16. Petrovic A, Alpdogan O, Willis LM, et al. LPAM (alpha 4 beta 7 integrin) is an important homing integrin on alloreactive T cells in the development of intestinal graft-versus-host disease. *Blood*. 2004;103:1542-1547.
17. De Rosa SC, Roederer M. Eleven-color flow cytometry: a powerful tool for elucidation of the complex immune system. *Clin Lab Med*. 2001;21:697-712.
18. Sallusto F, Lenig D, Forster R, Lipp M, Lanzavecchia A. 2 subsets of memory T lymphocytes with distinct homing potentials and effector functions. *Nature*. 1999;401:708-712.
19. Butcher EC, Picker LJ. Lymphocyte homing and homeostasis. *Science*. 1996;272:60-66.
20. Weninger W, Crowley MA, Manjunath N, von Andrian UH. Migratory properties of naive, effector, and memory CD8(+) T cells. *J Exp Med*. 2001;194:953-966.
21. Ngo VN, Tang HL, Cyster JG. Epstein-Barr virus-induced molecule 1 ligand chemokine is expressed by dendritic cells in lymphoid tissues and strongly attracts naive T cells and activated B cells. *J Exp Med*. 1998;188:181-191.
22. Lerner KG, Kao GF, Storb R, Buckner CD, Clift RA, Thomas ED. Histopathology of graft-vs.-host reaction (GvHR) in human recipients of marrow from HL-A-matched sibling donors. *Transplant Proc*. 1974;6:367-371.
23. Atkinson K. Bone-marrow and blood stem-cell transplantation. In: Berry CL, ed. *Transplantation Pathology: A Guide for Practicing Pathologists*. Current Topics in Pathology. Vol 92. New York, NY: Springer; 1999:107-136.
24. Heymer B, Bunjes D, Friedrich W. *Clinical and Diagnostic Pathology of Graft-Versus-Host Disease (GvHD)*. New York, NY: Springer; 2002.
25. Murai M, Yoneyama H, Ezaki T, et al. Peyer patch is the essential site in initiating murine acute and lethal graft-versus-host reaction. *Nat Immunol*. 2003;4:154-160.
26. Mora JR, Bono MR, Manjunath N, et al. Selective imprinting of gut-homing T cells by Peyer patch dendritic cells. *Nature*. 2003;424:88-93.
27. Johansson-Lindbom B, Svensson M, Wurbel MA, Malissen B, Marquez G, Agace W. Selective generation of gut tropic T cells in gut-associated lymphoid tissue (GALT): requirement for GALT dendritic cells and adjuvant. *J Exp Med*. 2003;198:963-969.
28. Stagg AJ, Kamm MA, Knight SC. Intestinal dendritic cells increase T cell expression of alpha4beta7 integrin. *Eur J Immunol*. 2002;32:1445-1454.
29. Mora JR, Cheng G, Picarella D, Briskin M, Buchanan N, von Andrian UH. Reciprocal and dynamic control of CD8 T cell homing by dendritic cells from skin- and gut-associated lymphoid tissues. *J Exp Med*. 2005;201:303-316.
30. Panoskaltis-Mortari A, Price A, Hermanson JR, et al. In vivo imaging of graft-versus-host-disease in mice. *Blood*. 2004;103:3590-3598.
31. Foster AE, Marangolo M, Sartor MM, et al. Human CD62L- memory T cells are less responsive to alloantigen stimulation than CD62L+ naive T cells: potential for adoptive immunotherapy and allodepletion. *Blood*. 2004;104:2403-2409.
32. Friedman JS, Alpdogan O, van den Brink MR, et al. Increasing T-cell age reduces effector activity but preserves proliferative capacity in a murine allogeneic major histocompatibility complex-mismatched bone marrow transplant model. *Biol Blood Marrow Transplant*. 2004;10:448-460.
33. Korngold R, Sprent J. Negative selection of T cells causing lethal graft-versus-host disease across minor histocompatibility barriers: role of the H-2 complex. *J Exp Med*. 1980;151:1114-1124.
34. Shlomchik WD, Couzens MS, Tang CB, et al. Prevention of graft versus host disease by inactivation of host antigen-presenting cells. *Science*. 1999;285:412-415.
35. Ermann J, Hoffmann P, Edinger M, et al. Only the CD62L+ subpopulation of CD4+CD25+ regulatory T cells protects from lethal acute GVHD. *Blood*. 2005;105:2220-2226.
36. Taylor PA, Panoskaltis-Mortari A, Swedin JM, et al. L-Selectin(hi) but not the L-selectin(lo) CD4+25+ T-regulatory cells are potent inhibitors of GVHD and BM graft rejection. *Blood*. 2004;104:3804-3812.